

Methane concentration and isotopic composition measurements with a mid-infrared quantum-cascade laser

A. A. Kosterev, R. F. Curl, and F. K. Tittel

Rice Quantum Institute, Rice University, Houston, Texas 77251-1892

C. Gmachl, F. Capasso, D. L. Sivco, J. N. Baillargeon, A. L. Hutchinson, and A. Y. Cho

Bell Laboratories, Lucent Technologies, 600 Mountain Avenue, Murray Hill, New Jersey 07974

Received August 3, 1999

A quantum-cascade laser operating at a wavelength of $8.1\ \mu\text{m}$ was used for high-sensitivity absorption spectroscopy of methane (CH_4). The laser frequency was continuously scanned with current over more than $3\ \text{cm}^{-1}$, and absorption spectra of the $\text{CH}_4\ \nu_4\ P$ branch were recorded. The measured laser linewidth was 50 MHz. A CH_4 concentration of 15.6 parts in 10^6 (ppm) in 50 Torr of air was measured in a 43-cm path length with ± 0.5 -ppm accuracy when the signal was averaged over 400 scans. The minimum detectable absorption in such direct absorption measurements is estimated to be 1.1×10^{-4} . The content of $^{13}\text{CH}_4$ and CH_3D species in a CH_4 sample was determined. © 1999 Optical Society of America

OCIS codes: 140.5960, 300.1030, 300.6320, 010.1280.

Infrared laser absorption spectroscopy is known to be an effective tool for monitoring atmospheric trace-gas species. The demonstrated sensitivity of this technique is several parts in 10^9 (ppb).¹ Applications of this method are limited mainly by the availability of convenient tunable sources in the spectroscopically important region from 3 to $20\ \mu\text{m}$. Recently developed quantum-cascade (QC) lasers^{2,3} have been demonstrated to be useful tunable single-frequency light sources for laser-based absorption spectroscopy. High-resolution spectroscopy of NO and NH_3 ,⁴ N_2O detection by use of wavelength-modulation spectroscopy,⁵ and NH_3 detection with photoacoustic spectroscopy⁶ have been reported.

Methane (CH_4) is also an important trace component in the atmosphere, because of its contribution to global warming as well as its role in complex feedback mechanisms in tropospheric and stratospheric chemistry.⁷ In this Letter we demonstrate the application of direct absorbance measurements with a QC laser to CH_4 detection. We have also measured the isotopic composition of a CH_4 sample. Isotope measurements are an important tool in establishing the origin of CH_4 , since various CH_4 sources have different isotopic signatures.⁷ As a by-product, the concentration of atmospheric water vapor was measured. Measurements of water-vapor concentration are of interest, for example, in volcanic emission studies⁸ and in determining water-vapor levels in natural-gas distribution systems.

In these experiments a QC laser designed for cw operation at cryogenic temperatures in the $8.1\text{-}\mu\text{m}$ region was used. A schematic of the experimental arrangement is depicted in Fig. 1. The laser was placed in a liquid- N_2 Dewar equipped with a broadband antireflection-coated ZnSe window. The laser current was supplied by a low-noise driver controlled by a function generator, which resulted in a sawtoothed current from 0.43 to 1.65 A. We used two

off-axis aluminum gold-coated parabolic mirrors and an uncoated BaF_2 lens to collimate the QC laser beam. The gas sample was placed in a 43-cm-long cell fitted with Brewster ZnSe windows. After passing through the cell, the laser radiation was collected by a fast room-temperature photovoltaic HgCdZnTe detector. The detector signal was amplified first by a dc to 200 MHz transimpedance preamplifier and subsequently by a low-noise preamplifier (Stanford Research Systems SR560). We set the bandwidth of the latter to dc to 100 kHz to decrease detector noise. The amplified signal was digitized with a National Instruments DAQCard-AI-16XE-50 data acquisition card with a laptop computer. This card can acquire as many as 200 ksamples/s with 16-bit resolution. All the spectra presented below result from averaging the signal over 400 current cycles at a 24-Hz repetition rate (8000 data points per cycle).

The detected infrared power as a function of laser current is shown in Fig. 2. Single-frequency lasing

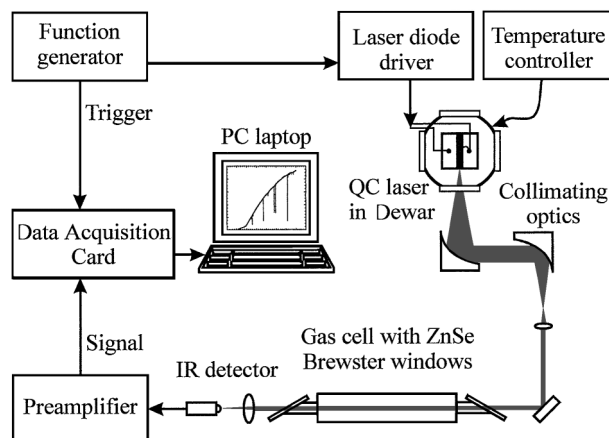


Fig. 1. Schematic of the experimental arrangement.

occurs at 0.51 A, with a slope efficiency of 2.6 mW/A, gradually increasing to 3.9 mW/A. A kink is clearly observable at 0.66 A on the power-current curve. The kink is caused by a second mode with a slope efficiency of 12.6 mW/A. The power of the first mode remains essentially constant at higher current. Therefore the laser power becomes concentrated mainly in the second mode, which we refer to as the strong mode.

The coexistence of two laser modes gives rise to extra spectral features in the absorption spectra [Fig. 3(b)] and to a false zero; i.e., the total absorption of one laser mode does not result in zero detector signal. However, concentration measurements are possible, because the power in each mode is well defined and reproducible. From Fig. 3 it is apparent that there is a good agreement between HITRAN database intensities and those derived from our measurements, which take into account two-frequency lasing. The frequency scale in Fig. 3 refers to the strong laser mode and was quadratically fitted to CH₄ line positions from HITRAN. The tuning of the weak mode was calibrated similarly. The frequency of each mode changes almost linearly with current, with slopes of -3.7 and -3.2 cm⁻¹/A for the strong and the weak modes, respectively. The separation between two modes is 1.43 cm⁻¹ at 0.6 A (the weak mode has a lower frequency).

In the spectral range covered by a frequency scan from 1240.5 to 1243.5 cm⁻¹ of the strong laser mode, five strong absorption lines and several weaker lines of CH₄ were observed. The strong lines belong to the *P* branch of the ν_4 bending mode. The assignment of lines in Fig. 3(a) is that made by Robiette.⁹ We used the spectrum recorded at 6.5-mTorr pressure of CH₄ [Fig. 3(b)] to determine the laser linewidth by comparison of the measured FWHM of the five strong lines with the Doppler-limited width. It was found that the laser linewidth is 50 ± 1.5 MHz, showing only small deviations from line to line. This result is in agreement with the results of Sharpe *et al.*,⁴ who reported linewidths of 40–85 MHz.

To estimate the sensitivity of the direct absorption technique with a QC laser source we acquired absorption spectra of CH₄-doped air samples at 50-Torr pressure. Figure 3(c) shows an example of such a spectrum. This spectrum was obtained by subtraction of the absorption spectrum of ambient air at 50 Torr from the spectrum of a CH₄-air mixture. This procedure enabled us to suppress substantially the baseline inhomogeneities, the weak interference fringes, and the broad pedestals resulting from water and CH₄ absorption in ambient air. The CH₄ concentration in the cell was derived from a comparison of the Voigt fit of the strongest observed line at 1240.995 cm⁻¹ with the line intensity predicted by HITRAN-based simulations. Both Doppler and Lorentzian widths in the fitting procedure were set to their predicted values. The calculations resulted in a peak absorption of $(0.162 \pm 0.005)\%$. This corresponds to a CH₄ concentration of 15.6 ± 0.5 ppm. To estimate the minimum detectable absorption we set the fitting procedure parameters to find a similar absorption feature centered at a frequency at which no real absorption lines are present. In such simulations the peak

absorption of this artificial line never exceeded 1.1×10^{-4} , and we assume this value to be the detection limit. Optical interference fringes are the principal sensitivity-limiting factor in these measurements. It should be noted that the line at 1240.995 cm⁻¹ is

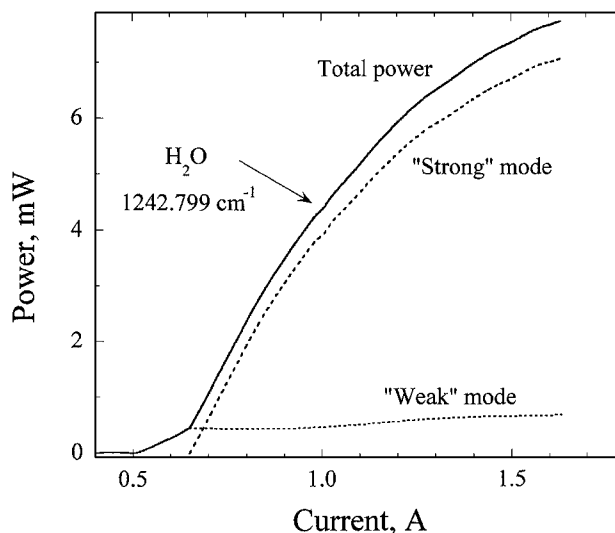


Fig. 2. Power on the detector versus QC laser current. The dip in the curve marked with the arrow is due to absorption by water vapor in the air. The dotted curves show power in each of the two laser modes.

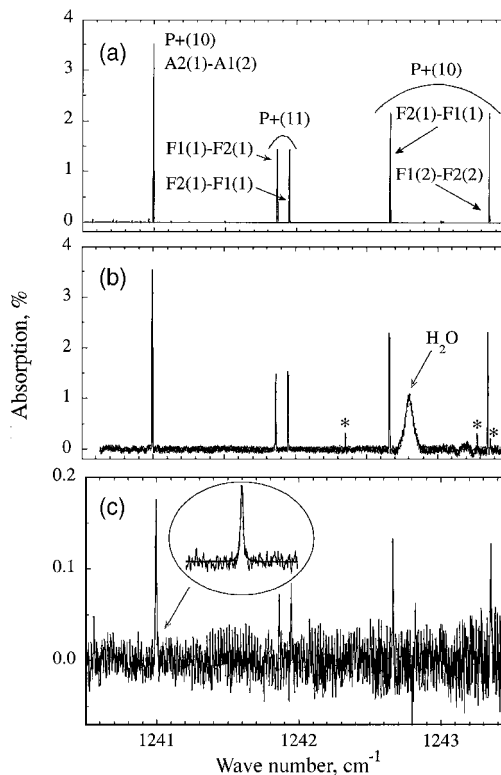


Fig. 3. (a) Simulated absorption spectrum of CH₄ (6.5 mTorr, 43 cm) and (b) measured spectrum for the same conditions. The false absorption lines that appear because of the two-mode lasing are marked with asterisks. (c) Measured spectrum of 20 ppm of CH₄ in 50 Torr of air. Inset, the Voigt fit of the strongest absorption line. The path length is 43 cm for all three spectra.

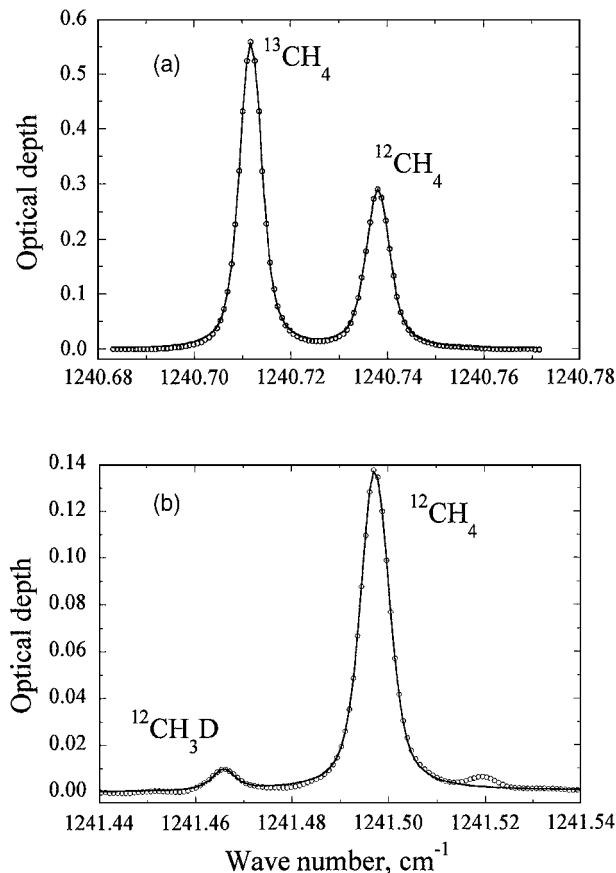


Fig. 4. (a) Absorption lines used to define the ^{13}C content in the CH_4 sample. (b) Absorption line of the deuterated CH_4 . The open circles represent the measured data, and the solid curves represent their Voigt fitting.

approximately six times weaker than the strongest lines in the same CH_4 absorption band (R branch). Therefore, selection of a QC laser operating at $\sim 1330\text{ cm}^{-1}$ would lead to an improvement in the minimum detectable concentration of CH_4 .

In addition to the absorption lines of the most-abundant isotopic species, $^{12}\text{CH}_4$, lines of both $^{13}\text{CH}_4$ and $^{12}\text{CH}_3\text{D}$ were also observed. To measure the isotopic composition of a sample we acquired the absorption spectrum with 16.9 Torr of CH_4 in the gas cell. We chose two pairs of lines for the isotopic measurements. In each case, one line corresponds to the less-abundant isotopic species and the other one to the $^{12}\text{CH}_4$ $2\nu_4-\nu_4$ hot band (Fig. 4). We selected the pairs to obtain two closely located (but not strongly overlapping) lines of comparable intensity and to avoid interference from the wings of the stronger absorption lines. The lines were fitted with a Voigt envelope, and the ratio of areas under each fitting curve was compared with the ratio predicted from HITRAN data. The relative line intensities in HITRAN are based on the isotopic composition with $\delta^{13}\text{C} = \delta\text{D} = 0\text{‰}$ corresponding to the V-SMOW standard for deuterium¹⁰ and the PDB standard for ^{13}C (Ref. 11) ($[\text{CH}_4^{13}]/[\text{CH}_4^{12}] = 1.12 \times 10^{-2}$ and $[\text{CH}_3\text{D}^{12}]/[\text{CH}_4^{12}] = 6.23 \times 10^{-4}$). Therefore, such a comparison provides $\delta^{13}\text{C}$ and δD values.

As a result of this procedure, we obtain for our CH_4 sample $\delta\text{D} = -220\text{‰}$ and $\delta^{13}\text{C} = +15\text{‰}$.

According to data available on the National Institute of Standards and Technology Web page,¹² a natural subsurface gas δD is typically in the -140‰ to -250‰ range, and $\delta^{13}\text{C}$ lies between -25‰ and -90‰ . Presumably, our CH_4 sample (Matheson UHP grade) has a similar isotopic signature. Several percent deviation of the measured $[\text{CH}_4^{13}]/[\text{CH}_4^{12}]$ ratio from the expected value may be caused by some inaccuracy in the line intensities from HITRAN, especially for hot bands. For more-reliable data it is necessary to use a calibrated reference sample with a known isotopic composition.

The broad spectral line in the spectrum shown in Fig. 3(b) is due to atmospheric water-vapor absorption. It corresponds to a weak line centered at 1242.799 cm^{-1} . A Lorentzian fit of this feature yields a 1.23% peak absorption. The water-vapor pressure is estimated to be 14.8 Torr, or 62% humidity, for a laser beam path in air of $\sim 137\text{ cm}$ at a temperature of $+25\text{ °C}$. This result is in agreement with hygrometer readings of 63%.

Financial support of the work performed by the Rice group was provided by NASA, the Texas Advanced Technology Program, the National Science Foundation, and the Welch Foundation. The Bell Laboratories team received partial support from the Defense Advanced Research Projects Agency—U.S. Army Research Office under grant DAA G 55-98-C-0050. A. Kosterev's e-mail address is akoster@rice.edu.

References

1. K. P. Petrov, S. Waltman, E. J. Dlugokencky, M. Arbore, M. M. Fejer, F. K. Tittel, and L. W. Hollberg, *Appl. Phys. B* **64**, 567 (1997).
2. F. Capasso, C. Gmachl, D. L. Sivco, and A. Y. Cho, *Phys. World* **12**, 27 (1999).
3. J. Faist, C. Gmachl, F. Capasso, C. Sirtori, D. L. Sivco, J. N. Baillargeon, and A. Y. Cho, *Appl. Phys. Lett.* **70**, 2670 (1997).
4. S. W. Sharpe, J. F. Kelly, J. S. Hartman, C. Gmachl, F. Capasso, D. L. Sivco, J. N. Baillargeon, and A. Y. Cho, *Opt. Lett.* **23**, 1396 (1998).
5. K. Namjou, S. Cai, E. A. Whittaker, J. Faist, C. Gmachl, F. Capasso, D. L. Sivco, and A. Y. Cho, *Opt. Lett.* **23**, 219 (1998).
6. B. A. Paldus, T. G. Spence, R. N. Zare, J. Oomens, F. J. M. Harren, D. H. Parker, C. Gmachl, F. Capasso, D. L. Sivco, J. N. Baillargeon, A. L. Hutchinson, and A. Y. Cho, *Opt. Lett.* **24**, 178 (1999).
7. P. Bergamaschi, M. Schupp, and G. W. Harris, *Appl. Opt.* **33**, 7704 (1994).
8. C. Oppenheimer, P. Francis, M. Burton, A. J. H. Maciejewski, and L. Boardman, *Appl. Phys. B* **67**, 505 (1998).
9. A. J. Robiette, *J. Mol. Spectrosc.* **86**, 143 (1981).
10. P. Fritz and J. Ch. Fontes, *Handbook of Environmental Isotope Geochemistry* (Elsevier, New York, 1980), Vol. 1, pp. 1–19.
11. H. Graig, *Geochim. Cosmochim. Acta* **12**, 133 (1957).
12. "NIST Database for the Isotopic Composition of Selected Atmospheric Constituents," <http://deuterium.nist.gov>.